PERGAMON

Available online at www.sciencedirect.com

SCIENCE DIRECT®

Polyhedron 22 (2003) 1837–1843

POLYHEDRON

www.elsevier.com/locate/poly

Polynitriles as ligands: new coordination polymers with the 1,1,3,3-tetracyano-2-ethoxypropenide ($tcnp^-$) bridging ligand

Franck Thétiot, Smaïl Triki *, Jean Sala Pala

UMR CNRS 6521, Université de Bretagne Occidentale, BP 809, 29285 Brest Cedex, France

Received 6 October 2002; accepted 10 December 2002

Abstract

New polymeric materials of formula $[M(tcnp)_2(H_2O)_2]$ ($M = Mn^{II}$, **1**; Fe^{II}, **2**; Co^{II}, **3** and Cu^{II}, **4**; $tcnp^- = [(NC)_2CC(OEt)C(CN)_2]^-$ = 1,1,3,3-tetracyano-2-ethoxypropenide anion) have been synthesized and characterized by infrared spectroscopy and X-ray crystallography. Crystal structures were determined for **1**, **3** and **4**. In these compounds, the organic ligand acts in a bridging mode with two of its four nitrogen atoms arising from the two different $C(CN)_2$ units; each metal ion has a centrosymmetric pseudo-octahedral *trans*-MN_4O_2 environment with four nitrogen atoms from four organic ligands and two oxygen atoms from water molecules. The octahedron, almost regular in **1** and **3**, is distorted in **4**, with a strong elongation along the pseudo fourfold axis. In all compounds (**1**–**4**), the molecular arrangement, which involves 16-membered $M(NCCCCCN)_2M$ dimetallacycles arising from the bridging mode of the organic ligand, can be described as chains of such dimetallacycles running along the [1−10] direction. Intra-chain M···M distances (9.017 Å in **1**, 8.887 Å in **3** and 9.133 Å in **4**) are significantly longer than those observed in the corresponding μ_2-bridging dicyanamide derivatives (≈ 7.4 Å); these large differences can be explained from the coordination mode of the μ_2-bridging tcnp ligand. Consequently, the shortest M···M distances are of the inter-chain type (8.282 Å in **1**, 8.245 Å in **3** and 8.120 Å in **4**); they occur along the [1 0 0] direction between metal ions of eclipsed chains and correspond to the *a* parameter. In the *ab* plane, the adjacent chains are connected by hydrogen bonds between the coordinated water molecules and one of the uncoordinated nitrogen atoms of the organic ligand, giving rise to 2D structures. For each compound, magnetic susceptibility measurements show a Curie law in the whole temperature range in agreement with the large separation between the paramagnetic ions.

Keywords: Coordination chemistry; Bridging ligand; Metallacycles; Coordination modes

1. Introduction

Polynitrile-transition metal compounds are of great current interest not only for their unusual magnetic properties but also for their intriguing architectures and topologies [1–8]. For geometrical and electronic reasons, the polynitrile units shown in Scheme 1 are interesting ligands for the construction of new extended molecular structures: (i) despite the presence of various CN units, their geometry preclude the possibility of a chelate coordination mode and they can only act as bridging ligands affording polymeric compounds [1,3–8], and (ii) association of the π electronic system of the CN groups with the π system of the central fragment induces high electronic delocalization and should allow transmission of electronic effects between the metal centers [1–4]. Following these general arguments, our objective is to examine the ability of these organic ligands to create a range of 1D, 2D and 3D polymeric assemblies [5,6]; this can also contribute to understand the binding modes of molecular systems such as binary ‘metal/tcnx’’ (x = e, q) compounds that present fascinating physical properties but for which the detailed

---

* Corresponding author. Tel.: +33-2-9801-6146; fax: +33-2-9801-7001.

E-mail address: smail.triki@univ-brest.fr (S. Triki).

0277-5387/03/$ - see front matter © 2003 Elsevier Science Ltd. All rights reserved.
doi:10.1016/S0277-5387(03)00150-5

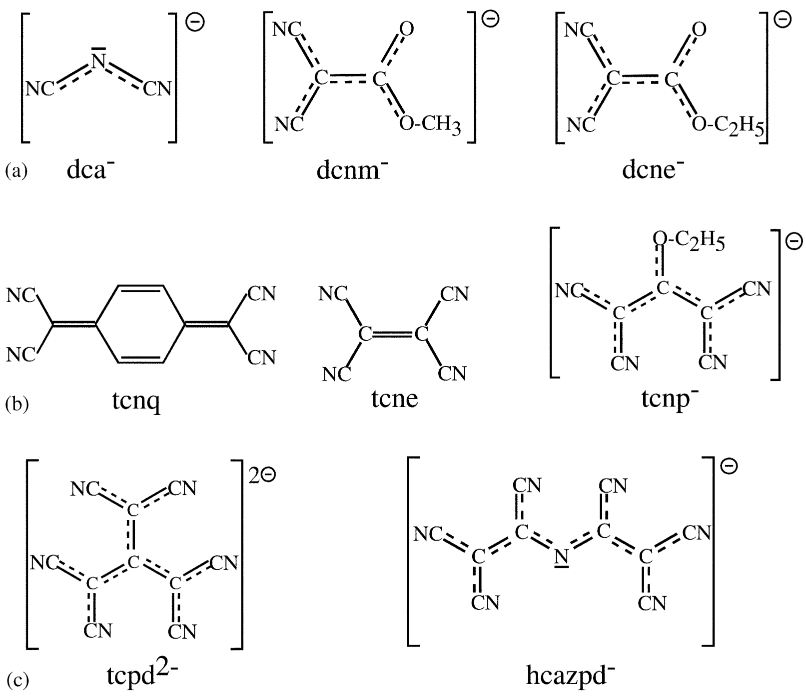

Scheme 1.

structures are as yet unknown [2]. In this context, we firstly reported two coordination polymers using respectively the Cu^{II}-$tcpd^{2-}$ and the Ag^{I}-$hcazpd^{-}$ systems (Scheme 1(c)) in which the two organic units act as μ_4-bridging ligands leading to two 3D-intriguing assemblies [5,6].

The first one, $[Cu(tcpd)(H_2O)_2]$, presents a structure generated by eclipsed chains which are laterally connected by equivalent eclipsed chains running orthogonally [5], while the second one, [Ag(hcazpd)], is generated from two different silver(I) ions, one of them having an unusual square-planar geometry [6]. Obviously, in these compounds, structural and physical properties are greatly affected by the number of the $C(CN)_2$ arms and by the structure of the central fragment of the anionic ligand; we therefore find interesting to study different ligands with varying the number of $C(CN)_2$ arms. Using the 2,2-dicyano-1-ethoxyethenolate anion ($dcne^- = [(NC)_2CC(O)OEt]^-$) and its methyl analogue ($dcnm^- = [(NC)_2CC(O)OMe]^-$) (Scheme 1(a)), i.e., ligands with a single $C(CN)_2$ unit and also having an oxygen atom able to act as a donor or to give hydrogen bonds, led us and Kremer et al. to new compounds whose structures are built from mono-dimensional chains of 12-membered dimetallacycles [9,10]. We now extend this work using a ligand containing two $C(CN)_2$ units as tcne or tcnq but separated by a central C(OEt) group, the 1,1,3,3-tetracyano-2-ethoxypropenide anion ($tcnp^- = [(NC)_2CC(OEt)C(CN)_2]^-$) (Scheme 1(b)). We report herein the syntheses, structural characterizations and magnetic properties of the new polymeric compounds of formula $[M(tcnp)_2(H_2O)_2]$ ($M = Mn^{II}$, **1**; Fe^{II}, **2**; Co^{II}, **3** and Cu^{II}, **4**).

2. Experimental

2.1. Materials

All reagents were purchased from commercial sources and used as received. 1,1-Diethoxy-2,2-dicyanoethene ($(NC)_2C{=}C(OEt)_2$) was first prepared according to the procedure previously reported by Middleton but this, in our hands, only gave a bad yield (5–10%) [11]. Since during this synthesis it has been observed that the time of heating is a crucial parameter, several syntheses were then performed with different heating times. The best procedure (58% yield) was described in Ref. [9]. Unless otherwise stated, reactions were performed under aerobic conditions.

2.2. Synthesis of potassium 1,1,3,3-tetracyano-2-ethoxypropenide K(tcnp)

A hot ethanolic solution (45 ml) of malononitrile ($CH_2(CN)_2$) (1.19 g, 18 mmol) and potassium *t*-butoxide (C_4H_9OK) (2.03 g, 18 mmol) was added to a warm ethanolic solution (60 ml) of 1,1-diethoxy-2,2-dicyanoethene (3.00 g, 18 mmol) and the mixture was refluxed for 2 h. On cooling, potassium 1,1,3,3-tetracyano-2-ethoxypropenide quickly precipitated as a white powder which was filtered on a sintered-glass and dried (3.12 g, 77% yield). *Anal*. Calc. for $KC_9H_5N_4O$: C, 48.20; H, 2.25; N, 24.98; K, 17.43. Found: C, 47.99; H, 2.24; N, 25.20; K, 17.52%. IR data (ν cm^{-1}): 3427br, 2205s, 1647w, 1499s, 1425m, 1379m, 1348m, 1187m, 999m.

2.3. Synthesis of compounds **1–4**

These compounds were prepared in the same way by treating saturated aqueous solutions of the corresponding metal chloride or metal sulfate with saturated solutions of potassium 1,1,3,3-tetracyano-2-ethoxypropenide in a tcnp/M ratio of two. The resulting solutions were heated for a few minutes with stirring and then left to stand. Slow evaporation of the solvent at room temperature gave crystals which all were satisfactory analysed for C, H, N with the formula $M(tcnp)_2(H_2O)_2$ (**1**, M = Mn; **2**, M = Fe; **3**, M = Co; **4**, M = Cu). **1**: Colourless crystals from $MnCl_2 \cdot nH_2O$. IR data (ν cm^{-1}): 3419br, 3331br, 2223s, 2200s, 1639w, 1475s, 1423m, 1381m, 1347m, 1191w, 1009w. **2**: Colourless crystals from $FeSO_4 \cdot 7H_2O$; in order to avoid oxidation of Fe^{II}, the synthesis was performed under nitrogen. IR data (ν cm^{-1}): 3375br, 3306br, 2223s, 2205s, 1646w, 1468s, 1422m, 1381m, 1345m, 1190w, 1010w. **3**: Orange crystals from $CoCl_2 \cdot 6H_2O$. IR data (ν cm^{-1}): 3404br, 3329br, 2230s, 2206s, 1616w, 1471s, 1421m, 1381m, 1344m, 1189w, 1010w. **4**: Orange crystals from $CuCl_2 \cdot 2H_2O$. IR data (ν cm^{-1}): 3326br, 3210br, 2254m, 2207s, 1479s, 1466s, 1421m, 1382m, 1346m, 1192w, 1010w.

2.4. Physical techniques

Infrared spectra were recorded in the range 4000–200 cm^{-1} as KBr pellets on a FT-IR NEXUS NICOLET Spectrometer. The magnetic studies were carried out on powder samples enclosed in medical caps. The magnetic susceptibility measurements were performed at 0.1 T after zero field cooling, in the temperature range 2–300 K with a SQUID magnetometer MPMS-XL-5 from Quantum Design. The molar susceptibility was corrected from the sample holder and diamagnetic contributions of all atoms (Pascal tables). Elemental analyses were obtained from the Service de microanalyses, CNRS, Gif sur Yvette, France.

2.5. X-ray crystallography

Cell parameters of compounds **1–4** given in Table 1 were obtained from single crystal diffraction. Preliminary studies showed that compounds **1–4** were isomorphic and therefore crystal data collections were only performed for **1**, **3** and **4** on a Nonius KappaCCD Diffractometer. The three structures were solved by direct methods and successive Fourier difference syntheses, and were refined on F by weighted anisotropic full-matrix least-squares methods [12]. The hydrogen atoms of compound **1** and that of the water molecule of compounds **3** and **4** were located by difference Fourier maps and refined isotropically, while the hydrogen atoms of the organic ligands of **3** and **4** were calculated [$d(C-H) = 0.95$ Å]; the thermal parameters were taken as $U_{iso} = 1.3\ U_{eq}(C)$ and therefore included as isotropic fixed contributors to F_c in the two structures. Scattering factors and corrections for anomalous dispersion were taken from the International Tables for X-ray Crystallography [13]. All calculations were performed on an Alphastation 255 4/233 computer. Pertinent crystal data, selected bond distances, selected bond angles of **1**, **3** and **4** are listed in Tables 1–3, respectively.

3. Results and discussion

3.1. Synthesis and IR spectroscopy

Potassium 1,1,3,3-tetracyano-2-ethoxypropenide K(tcnp) was prepared by reaction in ethanol of 1,1-diethoxy-2,2-dicyanoethene with malononitrile and potassium *t*-butoxide. Treatments of a saturated aqueous solution of K(tcnp) with saturated aqueous solutions of the corresponding metal salts (either hydrated MCl_2 or MSO_4) in a $tcnp^-/M(II)$ ratio of two gave, after slow evaporation, the new compounds $[M(tcnp)_2(H_2O)_2]$ ($M = Mn^{II}$, **1**; Fe^{II}, **2**; Co^{II}, **3** and Cu^{II}, **4**) [14]. The IR spectra of compounds **1–4** show similar patterns to that of the potassium salt K(tcnp). In each case, two strong absorption bands (2200 and 2223 cm^{-1} for **1**; 2205 and 2223 cm^{-1} for **2**; 2206 and 2230 cm^{-1} for **3**; 2207 and 2254 cm^{-1} for **4**) are assigned to the ν_{CN}. The first one is almost similar to that observed in the K(tcnp) spectrum containing the uncoordinated $tcnp^-$ moiety (2205 cm^{-1}), while the second is slightly shifted to higher wave-numbers. This is in good agreement with the presence of both coordinated and uncoordinated CN groups in the four compounds as shown by the X-ray structure. Broad features centered near 3400 cm^{-1} (ν_s and ν_{as}, OH) are indicative of the water molecules but do not allow to distinguish between free and coordinated water molecules.

3.2. Description of the structures $[M(tcnp)_2(H_2O)_2]$ ($M = Mn^{II}$ (*1*), Fe^{II} (*2*), and Cu^{II} (*4*)) and $[Co(tcnp)_2(H_2O)]$ (*3*)

Since preliminary studies indicated that compounds **1–4** are isomorphic, single crystal structure determinations were only performed on **1**, **3** and **4**. These compounds have a structure generated by a metal ion on special position (0, 0, 0), one organic ligand and a water molecule both in general positions (Fig. 1).

As expected, the organic ligand acts with a bridging coordination mode; this mode involves two nitrogen

Table 1
Crystal data for compounds **1**–**4**

Empirical formula	$C_{18}H_{14}N_8O_4Mn$ (**1**)	$C_{18}H_{14}N_8O_4Fe$ (**2**)	$C_{18}H_{14}N_8O_4Co$ (**3**)	$C_{18}H_{14}N_8O_4Cu$ (**4**)
Molecular weight [a]	461.30	462.21	465.30	469.90
Space group	$P\bar{1}$	$P\bar{1}$	$P\bar{1}$	$P\bar{1}$
a (Å)	8.2823(9)	8.2323(7)	8.2454(8)	8.1199(4)
b (Å)	8.4139(9)	8.4470(6)	8.4727(7)	8.6389(5)
c (Å)	9.2688(8)	9.1410(7)	9.286(1)	9.1507(6)
α (°)	83.02(1)	82.90(1)	80.85(1)	82.51(1)
β (°)	69.77(1)	69.92(1)	69.44(1)	69.45(1)
γ (°)	65.37(1)	64.63(1)	64.20(1)	65.96(1)
V (Å^3)	550.7	525.6	546.9	548.9
Z [a]	1	1	1	1
ρ_{calc} (Mg m^{-3})	1.391	1.460	1.413	1.422
μ (mm^{-1})	0.6129	0.755	0.820	1.034
Reflections unique/R_{int}	2163/0.023		2396/0.038	2454/0.020
Reflections with $I > 4\sigma(I)$	1580		1308	1471
N_v	170		150	150
$R(F_o)$ [b]/$R_w(F_o)$ [c]	0.030/0.042		0.038/0.057	0.027/0.038
Goodness-of-fit F^2 [d]	1.010		1.119	1.009
$\Delta\rho_{max,min}$ (e Å^3)	0.255/−0.276		0.662/−0.363	0.279/−0.264

[a] For all compounds **1**–**4**, the asymmetric unit contains 0.5 of the chemical formula.
[b] $R = \Sigma|F_o - F_c|/F_o$.
[c] $R_w = [\Sigma w(|F_o| - |F_c|)^2/w(F_o)^2]^{1/2}$.
[d] $GOF = [(\Sigma w|F_o| - |F_c|)^2/(N_{obs} - N_{var})]^{1/2}$.

Table 2
Selected bond lengths (Å) in compounds **1**, **3** and **4**

	1	3	4
M–N1	2.204(2)	2.105(3)	1.994(2)
M–N3	2.223(2)	2.106(3)	2.382(2)
M–O1	2.171(2)	2.083(3)	1.995(2)
C1–C5	1.412(2)	1.420(4)	1.415(2)
C2–C5	1.418(3)	1.428(5)	1.431(3)
C3–C6	1.411(2)	1.413(4)	1.412(3)
C4–C6	1.422(2)	1.425(4)	1.425(3)
C5–C7	1.402(2)	1.408(4)	1.406(3)
C6–C7	1.402(3)	1.409(4)	1.409(3)
C7–O2	1.332(2)	1.341(3)	1.340(2)
C8–O2	1.452(2)	1.445(5)	1.454(3)
C8–C9	1.493(3)	1.471(6)	1.464(5)

Table 3
Selected bond angles (°) in compounds **1**, **3** and **4**

	1	3	4
N1–M–N3	87.18(6)	86.9(1)	86.55(8)
N1–M–O1	89.85(6)	89.7(1)	89.65(8)
N3–M–O1	88.05(6)	88.9(1)	88.35(8)
C1–C5–C2	118.4(2)	118.5(3)	118.6(2)
C1–C5–C7	122.3(2)	121.6(3)	122.2(2)
C2–C5–C7	119.3(1)	119.8(3)	119.1(2)
C3–C6–C4	114.2(2)	115.0(3)	115.5(2)
C3–C6–C7	123.0(1)	122.8(3)	123.0(2)
C4–C6–C7	122.7(1)	122.1(3)	121.5(2)
C5–C7–C6	124.6(1)	124.9(2)	125.3(1)
C5–C7–O2	112.7(2)	112.5(3)	112.4(2)
C6–C7–O2	122.7(2)	122.6(3)	122.2(2)
C9–C8–O2	107.9(2)	108.6(4)	108.7(3)
C7–O2–C8	122.3(2)	123.1(3)	122.4(2)

atoms from cyano groups of the two different $C(CN)_2$ wings (Fig. 2). Each metal ion has a centrosymmetric *trans*-MN_4O_2 pseudo-octahedral geometry with four nitrogen atoms from four organic ligands and two oxygen atoms from water molecules (Fig. 1). For the Mn and Co compounds (**1** and **3**), the octahedron is only very slightly distorted since the six M–L bond lengths range from 2.171 to 2.223 Å for **1** and from 2.083 to 2.106 Å for **3**, and bond angles from 87.2 to 92.8° for **1** and from 86.9 to 93.1° for **3** (Tables 2 and 3). For the Cu compound (**4**) very strong deformations are observed: the Cu octahedron may be viewed as a planar array of four short Cu–L bonds (Cu–O1 1.995 and Cu–N1 1.994 Å) with two *trans* long ones (Cu–N3 2.382 Å) and bond angles from 86.5 to 93.5° (Tables 2 and 3). As shown in Fig. 2, the structure involves 16-membered $(M(NCCCCCN)_2M)$ dimetallacycles since two bridging tcnp ligands connect two M(II) ions. Theses dimetallacycles are connected each other through the metal ions to give a mono-dimensional chain running along the [1 −1 0] direction (Fig. 2). Careful examination of the extended structure shows that the intra-chain M···M distances (9.017 Å in **1**, 8.887 Å for **3** and 9.133 Å in **4)** are significantly longer than those observed for the corresponding dca and dcne (Scheme 1(a)) derivatives (< 7.4 Å) [3,4,9]. These large differences can be explained from the coordination modes of the μ_2-bridging polynitrile ligands; the dca and dcne coordination

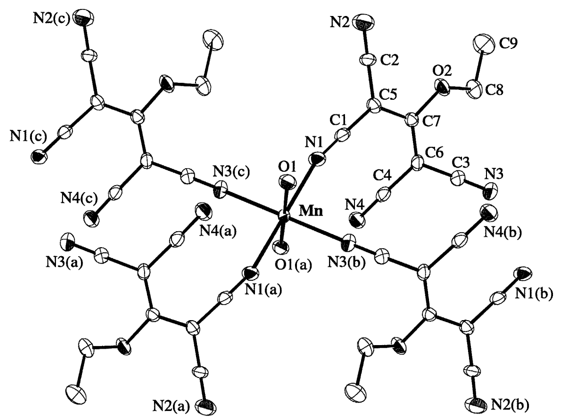

Fig. 1. ORTEP view showing the asymmetric unit, the atom labeling scheme and metal environment in compound **1** (similar asymmetric unit in compounds **3** and **4**). Code of equivalent positions: (a) $-x$, y, $-z$; (b) $-1-x$, $1-y$, $-z$ and (c), $1+x$, $-1+y$, z.

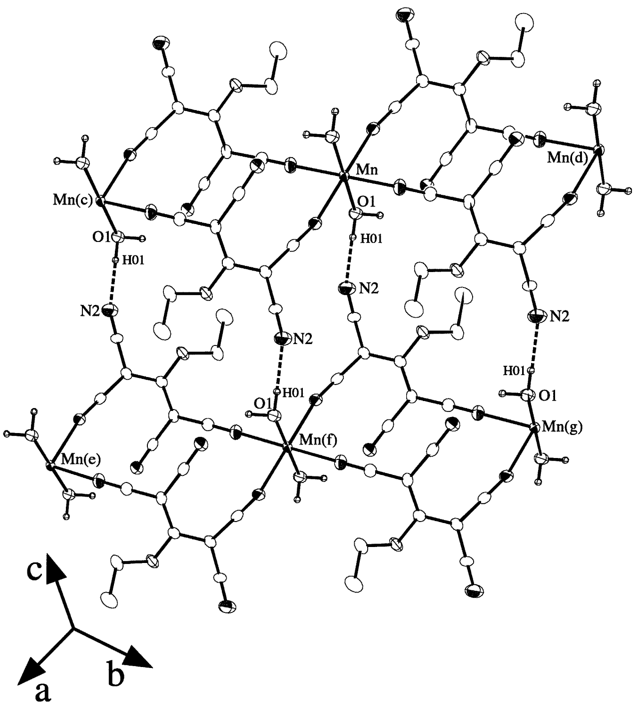

Fig. 2. ORTEP view of two equivalent adjacent chains showing hydrogen bonds in **1** (similar Figures for compound **3** and **4**). Fractional coordinates: Mn: (0 0 0); Mn(c): (1 −1 0); Mn(d): (−1 1 0); Mn(e): (0 1 1); Mn(f): (−1 0 1) and Mn(g): (−2 1 1).

compounds involve 12-membered dimetallacycles [M(NCXCN)$_2$M] (X = N for dca; X = CO(OEt) for dcne], while structures **1**–**4** involve 16-membered [M(NCCCCCN)$_2$M] dimetallacycles since two metal ions are connected via two different C(CN)$_2$ wings of the same bridging tcnp ligand. Therefore, it is not surprising that the shortest M···M distances are of the inter-chain type; they occur along the [1 0 0] direction between metal ions of eclipsed chains and correspond to the *a* parameter (8.282 Å in **1**, 8.245 Å in **3** and 8.120 Å in **4**). In the *ab* plane, the adjacent equivalent chains are connected by hydrogen bonds between the coordinated water molecules and one of the uncoordinated nitrogen atoms of the organic ligand (in **1** O1···N2: 2.846 Å, N2···H–O1 174.1°; in **3** O1···N2: 2.846 Å, N2···H–O1 177.3° and in **4** O1···N2: 2.828 Å, N2···H–O1 174.4°) giving rise to 2D structures (Fig. 2).

In summary, the extended molecular structures of compounds **1**–**4** are essentially equivalent, the main difference lying in the geometric deformations of the coordination polyhedron in compound **4** by respect to the perfect octahedron.

3.3. Tcnp as ligand

Obviously, the central carbon atoms of the ligand (C5, C6 and C7) are sp^2 hybridised (sums of bond angles around each atom = 360.0 or 359.9°) (Fig. 1 and Table 3). Due to the presence of the supplementary π electron systems of the cyano groups, the ligand presents a strong electronic delocalization as indicated by the six almost equivalent C–C bond lengths (ranging from 1.402(2) to 1.422(2) in **1**, from 1.408(4) to 1.428(5) Å in **3** and from 1.406(3) to 1.431(3) Å in **4**). This delocalization includes the C7–O2 bond which is approximately 0.10–0.12 Å shorter than the single C8–O2 bond. Therefore, the tcnp ligand can be considered as a resonance hybrid of the different canonical structures given in Scheme 2.

These forms, and the symmetrical ones not shown on the Scheme, give rise to the mean electronic structure of Scheme 3 which well agrees with the bond lengths and bond angles.

However, it is noteworthy that, despite this high conjugation, the organic ligand deviates significantly from planarity since the two almost planar C(CN)$_2$ wings are tilted out of the plane containing the central fragment C5C6C7O2 (Fig. 3) (in **1** tilt angles 15.7 and 19.2, dihedral angles between the two wings 31.2, similar values in **3**: 15.8, 20.2 and 32.7° and in **4**: 15.8, 17.9 and 30.9°, respectively).

3.4. Magnetic properties

Magnetic data for **1**–**4** in the form of $\chi_m T$ product vs. T (χ_m being the molar magnetic susceptibility per mole of M(tcnp)$_2$(H$_2$O)$_2$) are depicted in Fig. 4.

All compounds exhibit similar behavior; the values of $\chi_m T$ remain essentially constant at high temperatures, with room temperature values of 4.50, 3.31, 2.98, 0.42 emu K mol^{-1} for **1**–**4** respectively. The values of compounds **1**, **2** and **4** are in good agreement with the expected magnitude for the corresponding magnetically isolated paramagnetic ions, $S = 5/2$, $S = 2$ and $S = 1/2$ respectively. However, the value obtained for compound **3** (2.98 emu K mol^{-1}) is greater than that calculated for the spin only case (1.87 emu K mol^{-1}), indicative of a

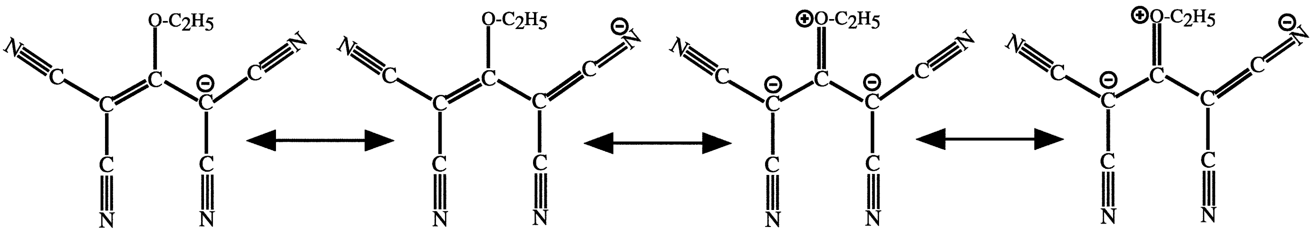

Scheme 2.

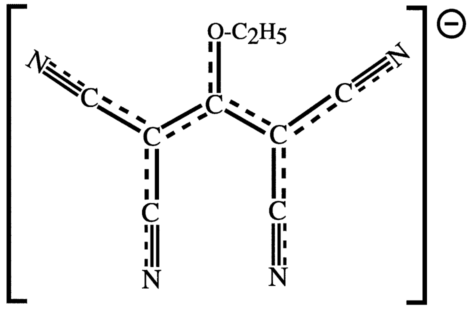

Scheme 3.

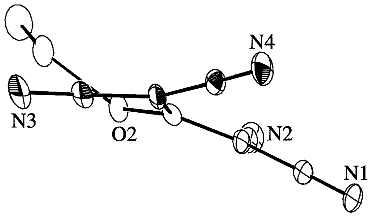

Fig. 3. Structure of the tcnp anion in **1** showing the tilt, out of the central plane, of the almost planar $C(CN)_2$ wings.

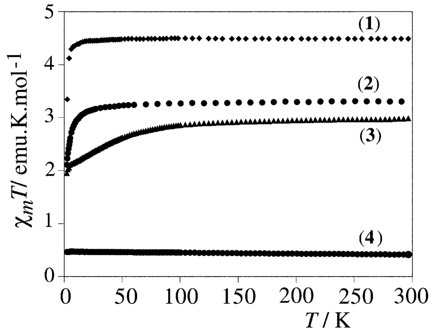

Fig. 4. Thermal variations of the magnetic susceptibility in the forms $\chi_m T$ vs. T for **1**–**4**.

significant orbital contribution of the isolated Co^{II} ion. For **1**, the $\chi_m T$ value remains constant when cooling down up to 16 K, then decreases sharply at low temperature reaching a value of 3.34 emu K mol^{-1}, while for **4** it remains constant up to 2 K. For **3**, the $\chi_m T$ value exhibits a continuous decrease upon cooling to reach a value of 1.94 emu K mol^{-1} at 2 K, this behaviour is most likely due to the single anisotropy of Co^{II} ions. Finally, for compound **2** the initial magnetic measurements on randomly oriented polycrystalline samples showed an increase in the $\chi_m T$ product at low temperature; when cooling below 50 K this product increases and reaches a maximum of 4.5 emu K mol^{-1} at 5 K. These effects, which are due to the anisotropy of the susceptibility of the sample, have already been observed in Fe(II) and Mn(III) compounds [9,15]. In order to remove them, new measurements were done on pressed pellets to prevent crystallite torquing. In these conditions, the magnetic behavior of **2**, depicted in Fig. 4, in the form of $\chi_m T$ product vs. T, remains constant down 50 K and then decreases rapidly to 2.05 emu K mol^{-1} at 2 K because essentially the zero field splitting effects.

No susceptibility maximum is observed in the whole temperature range explored (2–300 K), this can be understood taking into account the large separation between the paramagnetic ions in all compounds (> 9.0 Å) which are imposed by the two –NCCCCCN– bridges connecting the metal centers.

4. Conclusion

This study, which concerns a new series of mono-dimensional polynitrile-transition metal compounds, shows that the 1,1,3,3-tetracyano-2-ethoxypropenide anion $[(NC)_2CC(OEt)C(CN)_2]^-$ acts with a μ_2-bridging coordination mode arising from one nitrogen atom from every $C(CN)_2$ wing. The molecular arrangement involves mono-dimensional chains of 16-membered dimetallacycles. The low dimensionality of these polymeric compounds is essentially caused by the presence of coordinated water molecules which reduces the number of M-tcnp coordinated sites around the metal ions; this prevents the coordination of the four nitrile groups. In an effort to increase the dimensionality of these materials, we are turning to syntheses in non-aqueous media, using organic solvents and the tetraethylammonium salt of the polynitrile instead of the potassium salt.

5. Supplementary material

Crystallographic data (excluding structure factors) for the structures of compounds **1**, **3** and **4** have been deposited with the Cambridge Crystallographic Data Centre as supplementary publication Nos. CCDC-190678 (**1**), CCDC-190679 (**2**) and CCDC-190680 (**3**). Copies of the data can be obtained free of charge on application to The Director, CCDC, 12 Union Road, Cambridge, CB2 1EZ, UK (fax: +44-1223-336033; e-mail: deposit@ccdc.cam.ac.uk or www: http://www.ccdc.cam.ac.uk).

Acknowledgements

This work was supported by CNRS (Centre National de la Recherche Scientifique, UMR 6521) and the University of Brest (SUCRI 2E). F.T. thanks the 'Ministère de l'Education Nationale, de la Recherche et de la Technologie' for postgraduate grant. We gratefully acknowledge Prof. J. Fischer and Dr A. De Cian (University of Strasbourg, France) for X-ray data collection and Dr P. Molinié (Institut des Matériaux, Nantes) for magnetic measurements.

References

[1] (a) K.R. Dunbar, Angew. Chem., Int. Ed. 35 (1996) 1659;
(b) J.S. Miller, J.L. Manson, Acc. Chem. Res. 34 (2001) 563.

[2] (a) R.A. Heintz, H. Zhao, X. Ouyang, G. Grandinetti, J. Cowen, K.R. Dunbar, Inorg. Chem. 38 (1999) 144;
(b) S.A. O'Kane, R. Clérac, H. Zhao, X. Ouyang, J.R. Galán-Mascarós, R. Heintz, K.R. Dunbar, J. Solid State Chem. 152 (2000) 159;
(c) H. Zhao, R.A. Heintz, X. Ouyang, K.R. Dunbar, C. Campana, R.D. Rogers, Chem. Mater. 11 (1999) 736;
(d) A. Rockenbauer, G. Speier, L. Szabó, Inorg. Chim. Acta 201 (1992) 5.

[3] (a) S.R. Batten, P. Jensen, C.J. Kepert, M. Kurmoo, B. Moubaraki, K.S. Murray, D.J. Price, J. Chem. Soc., Dalton Trans. (1999) 2987;
(b) M. Kurmoo, C.J. Kepert, Mol. Cryst. Liq. Cryst. 334 (1999) 693;
(c) M. Kurmoo, C.J. Kepert, New J. Chem. 22 (1998) 1515.

[4] (a) C.R. Kmety, J.L. Manson, Q.-Z. Huang, J.W. Lynn, R.W. Erwin, J.S. Miller, A.J. Epstein, Mol. Cryst. Liq. Cryst. 334 (1999) 631;
(b) J.L. Manson, C.R. Kmety, A.J. Epstein, J.S. Miller, Inorg. Chem. 38 (1999) 2552;
(c) J.L. Manson, C.R. Kmety, Q.-Z. Huang, J.W. Lynn, G. Bendele, S. Pagola, P.W. Stephens, A.J. Epstein, J.S. Miller, Chem. Mater. 10 (1998) 2552;
(d) J.L. Manson, E. Ressouche, J.S. Miller, Inorg. Chem. 39 (2000) 1135;
(e) J.L. Manson, Q.-Z. Huang, J.W. Lynn, H.-J. Koo, M.-H. Whangbo, R. Bateman, T. Otsuka, N. Wada, D.N. Argyriou, J.S. Miller, J. Am. Chem. Soc. 123 (2001) 162.

[5] (a) S. Triki, J. Sala Pala, M. Decoster, P. Molinié, L. Toupet, Angew. Chem., Int. Ed. 38 (1999) 113;
(b) S. Triki, J. Sala Pala, A. Riou, P. Molinié, Synthetic Met. 102 (1999) 1472.

[6] M. Decoster, J.E. Guerchais, Y. Le Mest, J. Sala Pala, S. Triki, L. Toupet, Polyhedron 15 (1996) 195.

[7] (a) S.R. Batten, B.F. Hoskins, R. Robson, Angew. Chem., Int. Ed. 36 (1997) 636;
(b) J.H. Enemark, R.H. Holm, Inorg. Chem. 3 (1964) 1516;
(c) S.R. Batten, B.F. Hoskins, R. Robson, Chem. Commun. (1991) 445;
(d) J.L. Manson, C. Campana, J.S. Miller, Chem. Commun. (1998) 251.

[8] (a) S.R. Batten, A.R. Harris, P. Jensen, K.S. Murray, A. Ziebell, J. Chem. Soc., Dalton Trans. (2000) 3829;
(b) P. Jensen, D.J. Price, S.R. Batten, B. Moubaraki, K.S. Murray, Chem. Eur. J. 6 (2000) 3186.

[9] F. Thétiot, S. Triki, J. Sala Pala, C.J. Gómez-García, J. Chem. Soc., Dalton Trans. (2002) 1687.

[10] C. Kremer, C. Melián, J. Torres, M.P. Juanicó, C. Lamas, H. Pezaroglo, E. Manta, H. Schumann, J. Pickardt, F. Girgsdies, O.N. Ventura, F. Lloret, Inorg. Chim. Acta 314 (2001) 83.

[11] W.J. Middleton, V.A. Engelhardt, J. Am. Chem. Soc. 80 (1958) 2788.

[12] C.K. Fair, MOLEN, An Interactive Intelligent System for Crystal Structure Analysis, User Manual, Enraf-Nonius, Delft, The Netherlands, 1990.

[13] D.T. Cromer, J.T. Waber (Eds.), International Tables for X-Ray Crystallography, vol. 4, Kynoch Press, Birmingham, UK, 1975.

[14] From the same procedure used for the syntheses of **1**–**4**, the Ni(II) analogue was also obtained, but its structure could not be obtained since the sample was a powder. However, the infrared pattern of the compound is similar to that of compounds **1**–**4**, and its elemental analyses is in good agreement with $[Ni(tcnp)_2(H_2O)_2]$ formula. The $\chi_m T$ value, of 1.35 emu K mol^{-1} at room temperature, remains constant when cooling down up to 13 K, then decreases sharply at low temperature reaching a value of 0.82 emu K mol^{-1} at 2 K. *Anal*. Calc. for $C_{18}H_{14}N_8O_4Ni$: C, 46.49; H, 3.03; N, 24.09; Ni, 12.62%. Found: C, 45.90; H, 3.11; N, 23.56; Ni, 12.57%. IR data (ν cm^{-1}): 3419br, 3332br, 2219s, 2199s, 1632w, 1469s, 1420m, 1376m, 1340m, 1189w, 1010w.

[15] (a) S.R. Batten, P. Jensen, B. Moubaraki, K.S. Murray, Chem. Commun. (2000) 2331;
(b) B.J. Kennedy, K.S. Murray, Inorg. Chem. 24 (1985) 1552.